Estimation of Multipath Fading Channel Using Fractal Based VSLMS Algorithm

ANUBHA GUPTA[1] and SHIVDUTT JOSHI[2]
Deptt. of Electronics and Communication Engineering[1] and Electrical Engineering Department[2]
IIIT-Delhi[1] and Indian Institute of Technology-Delhi[2],
Delhi, India[1] and Hauz Khas, Delhi-110016, India[2].
anubha@iiitd.ac.in[1], sdjoshi@ee.iitd.ac.in[2]

Abstract: — This paper evaluates the performance of fractal based variable step-size LMS (FB-VSLMS) algorithm on the estimation of multipath fading channel for nonstationary process transmission. The algorithm exploits the statistics of the nonstationary process and uses non-diagonal step-size matrix to design an adaptive LMS filter in order to estimate slow fading correlated Rayleigh channel, in particular, asymptotically stationary AR channel and Jakes channel. Analytic expressions of steady-state mean-square weight error (MSWE) and optimum step-size parameter are computed for these channels. The analytical expression of optimum step-size would enable reliable channel estimation in real time. Simulation results are compared with analytic expressions developed in this paper and are shown to agree with good conformity.

Keywords:- Rayleigh fading channel, channel estimation, variable step-size LMS algorithm, nonstationary signals.

1 Introduction

In mobile radio communication, estimation of a time-varying channel is an area of active research. In a wireless channel, channel characteristics vary with time due to multipath fading. Thus, it is important for any LMS based algorithm on channel modeling to track the time-varying channel characteristics. Multipath fading has two effects: large-scale fading due to motion over large areas and small-scale fading due to small changes in position [1]. While large-scale fading is more relevant for cell-site planning, small-scale fading is more relevant for the design of efficient communication system such as channel equalization [2]. One of a very useful time-varying channel model in wireless communication is the Rayleigh channel model that is based on small-scale fading [2]. In this paper, we have considered the small-scale fading effect caused by a randomly time varying channel that leads to slow fading.

There have been a number of research studies on the estimation of multipath fading channel [3-9]. However, most of the research studies have considered stationary signal transmission over these channels. Some studies have considered transmission of 1st order fractional Brownian motion (nonstationary process) over time invariant and time-varying channels [10-11]. Because the orthogonal wavelet transform is assumed to mitigate [12-14] the nonstationary attribute of the signal, these studies have first used wavelet analysis filtering, designed adaptive filter for each of the subband and then, computed the inverse wavelet transform to restore the signal [10-11]. As a consequence, instead of designing one adaptive filter, there is a need to design a bank of adaptive filters, one corresponding to each subband. Also, the processing overhead increases because of the computation of forward and inverse wavelet transform, which is a critical issue in real time applications. This drawback provides us the motivation for exploring a channel estimation strategy that is naturally suited for a class of nonstationary signal transmission.

In [15], Gupta et. al. presented an fBm based variable step-size LMS (FB-VSLMS) algorithm for tracking signals from a class of Gaussian $1/f^{\beta}$ family of fractal signals, namely 1st order fractional Brownian motion, that are inherently nonstationary. In this paper, we have investigated the performance of this algorithm to estimate asymptotically stationary AR channels and Jakes channel that are examples of Gaussian Wide-sense Stationary Uncorrelated Scattering (WSSUS) channel model [19, 20]. Following are the salient features of this work: 1) we deal with multipath channel estimation for a specific class of Gaussian family of nonstationary signals as input to the channel. Instead of processing the input signal to mitigate the effect of non-stationarity and designing multiple adaptive filters in the wavelet domain, we exploit the statistics of the nonstationary process to design a single adaptive variable step-size LMS filter for channel estimation; 2) we use a non-diagonal step-size matrix which is simultaneously diagonalizable with the auto-covariance matrix of the input signal vector in the decoupled weight vector space; 3) we compute analytical expression of optimum step-size that would enable reliable channel estimation in real time; and 4) the available algorithms compute the range of step-size parameters by assuming the input signal to be stationary and ergodic while the statistical properties of the fractal signals required for the proposed fractal-based VSLMS (FB-VSLMS) algorithm can be completely characterized by estimating the single parameter i.e., the Hurst exponent.

The paper is organized as follows: In section 2, we review the fBm based variable step-size LMS (FB-VSLMS) algorithm in brief. In section 3, we present the analysis to estimate time-varying channels using FB-VSLMS algorithm. We also compute the expressions of steady-state mean-square weight error (MSWE) and optimum step-size in this section. Section 4 presents numerical results to validate the analysis. Simulation results are compared with analytic expressions derived in section 3. In the end, some concluding remarks are presented in Section 5.

Notations: We use lowercase bold letters and uppercase bold letters to represent vectors and matrices, respectively. The scalar variables are represented by lowercase italicized letters. In addition, $(\cdot)^*$ denotes Hermitian conjugation of a vector or a matrix, $(\cdot)^T$ denotes the transpose of $(\cdot)$, $\mathrm{Tr}(\cdot)$ is used to denote the trace of $(\cdot)$, and $\mathrm{E}(\cdot)$ denotes the expectation operator.

2 Brief Review of Fractal Based Variable Step-Size LMS (FB-VSLMS) Algorithm

The aim of this section is to present the FB-VSLMS algorithm in brief [15]. To this end, consider an adaptive linear combiner (ALC) of Fig.1 which is used to estimate the desired signal $d(n)$. The input to the ALC is a signal $\mathbf{x}(n) = [x(n)\ x(n-1)\ \ldots.\ x(n-N+1)]^T$, where $x(n)$ represents a sample function of a discrete-time fractional Brownian motion (fBm), also known as a fractal, with Hurst exponent (H) belonging to the range $0<H<1$ [16].

The weight vector update process of the LMS algorithm is given by

$$\mathbf{w}(n+1) = \mathbf{w}(n) + \boldsymbol{\alpha}(n)\mathbf{x}(n)e^*(n), \quad (1)$$

where $\mathbf{w}(n) = [w_0(n)\ w_1(n)\ \ldots.\ w_{N-1}(n)]^T$ is the weight vector of length N of ALC, $e(n) = d(n) - \hat{d}(n)$ is the output error, $\hat{d}(n) = \mathbf{w}^*(n)\mathbf{x}(n)$ is the ALC output and $\boldsymbol{\alpha}(n)$ is the algorithm step-size matrix. Because the input process is non-stationary; the step-size matrix used is a function of n. Here, it is to note that $\boldsymbol{\alpha}(n)$ is a non-diagonal matrix and is chosen to be simultaneously diagonalizable with the auto-covariance matrix $\mathbf{R}(n)$ of the input signal [15]. Thus, the same ordered orthonormal basis that diagonalizes the auto-covariance matrix $\mathbf{R}(n)$ of the input signal diagonalizes the step-size matrix $\boldsymbol{\alpha}(n)$ [15].

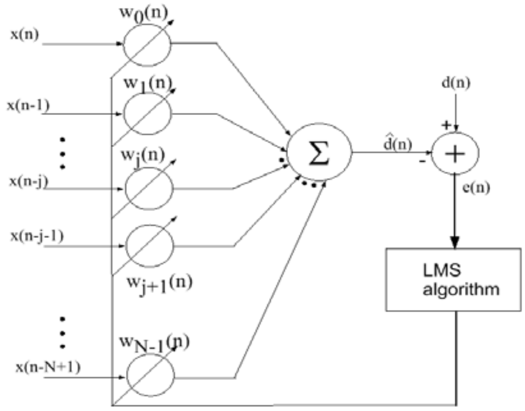

Fig.1: Adaptive Linear Combiner

Following assumptions are used in the FB-VSLMS algorithm:

AS1) The step-size matrix can be diagonalized using a unitary transformation that also diagonalizes the auto-covariance matrix of the input signal. This implies that

$$\boldsymbol{\alpha}(n)=\mathbf{Q}\boldsymbol{\Lambda}_{\alpha}(n)\mathbf{Q}^T, \quad (2)$$

where $\boldsymbol{\Lambda}_{\alpha}(n)= \mathrm{diag}\{\alpha_1(n), \alpha_2(n),\ldots., \alpha_{N-1}(n), \alpha_N(n)\}$.

This matrix $\mathbf{Q}$ is an orthogonal matrix that diagonalizes the auto-covariance matrix $\mathbf{R}(n)$ of the input signal. Because of the specific choice of $\boldsymbol{\alpha}(n)$ as stated above, it transforms the filter co-ordinate space such that update of one weight coefficient does not affect other weight coefficients [17]. The diagonal matrix $\boldsymbol{\Lambda}_{\alpha}(n)$ defines the step-size parameters to be used with different weights in this transformed space and transforms to $\boldsymbol{\alpha}(n)$ in the original filter weight co-ordinate space using $\mathbf{Q}$ in (2).

AS2) $\mathbf{x}(n)$, $\mathbf{v}(n)$ and $e_0(n)$ are independent, where $\mathbf{v}(n)$ is the deviation in weights from the optimum and $e_0(n)$ is the zero mean Gaussian error at the minimum point.

At the global minima point, Wiener-Hopf solution for the optimum weight vector $\mathbf{w}_*$ is given by

$$\mathbf{R}(n)\mathbf{w}_* = \mathbf{p}(n), \quad (3)$$

and
$$e_0(n) = d(n) - \mathbf{w}_*^*\mathbf{x}(n), \quad (4)$$

where $\mathbf{R}(n)$ = E[$\mathbf{x}(n)\mathbf{x}^*(n)$] is the auto-covariance matrix of the input signal vector $\mathbf{x}(n)$, and $\mathbf{p}(n)$=E[$d(n)\mathbf{x}^*(n)$] is the cross correlation vector of the input signal vector $\mathbf{x}(n)$ and the desired signal $d(n)$.

To simplify for $\mathbf{R}(n)$, the algorithm uses the theorem proposed on the structure of auto-covariance matrix of discrete-time fractional Brownian motion [18]. This theorem, for ready reference, is reproduced below.

Theorem 1: The N x N auto-covariance matrix $\mathbf{R}(n)$ of a discrete-time 1st order fractional Brownian motion, with $0<H<1$, admits the following representation:

$$\mathbf{R}(n) = \mathbf{Q}(n)\mathbf{\Lambda}(n)\mathbf{Q}^{\mathrm{T}}(n)$$

For large n, $\mathbf{R}(n)$ can be approximated as $\hat{\mathbf{R}}(n)$ such that

$$\hat{\mathbf{R}}(n) = \mathbf{Q}\hat{\mathbf{\Lambda}}(n)\mathbf{Q}^{\mathrm{T}}, \quad (5)$$

where $\mathbf{Q}(n) \approx \mathbf{Q}$ is a constant orthogonal matrix and $\hat{\mathbf{\Lambda}}(n)$ = diag{$\lambda_1, \lambda_2, \ldots, \lambda_{N-1}, \lambda_N(n)$} for large n.

Note that all these eigenvalues of $\mathbf{R}(n)$ are independent of the time index n for large n except for $\lambda_N(n)$. All these eigenvalues depend on the Hurst exponent H characterizing the discrete-time fractional Brownian motion. The largest eigenvalue is a function of time index n and Hurst exponent H. This eigenvalue is modeled as [18]

(i) for $H <$ **Error!**,

$$\lambda_N(n) = \frac{\sigma_H^2}{2}\left[2Nn^{2H} + 2Hn^{2H-1}N(N-1) - \frac{2}{N}\sum_{i=1}^{N-1} i(N-i)^{2H}\right]$$

;

(ii) for $H >$ **Error!**,

$$\lambda_N(n) = \frac{\sigma_H^2}{2}\left[2Nn^{2H} + 2Hn^{2H-1}N(N-1)\right] + \frac{\sigma_H^2}{2}\left[-\frac{2}{N}\sum_{i=1}^{N-1} i(N-i)^{2H} + 2H^2n^{2H-2}\,\frac{N(N^2-1)}{12}\right]. \quad (6)$$

with σ_H^2 = **Error!**as given in [16].

From the above theorem, we note that the structure of auto-covariance matrix of the input fractal signal depends only on the Hurst exponent of the input signal. Thus, unlike other VSLMS algorithms, signal statistics in FB-VSLMS algorithm are estimated using a single parameter H. This helps in choosing step-sizes for different weights of ALC. All the time-invariant eigenvalues of $\mathbf{R}(n)$ are tabulated in [18] that can be selected without any computation while the last time-varying eigenvalue can be computed using (6). Thus, the valid ranges of all step-size parameters are determined by estimating only the Hurst exponent H of the input fractal process. The fixed unitary matrix $\mathbf{Q}$ are also tabulated in [18] for different sizes of the auto-covariance matrices and is available for ready reference. The same unitary matrix is used to form the step factor matrix $\boldsymbol{\alpha}(n)$ in (AS1) to be used in the proposed FB-VSLMS algorithm for channel estimation.

For the adaptive linear combiner in Fig. 1, it is shown in [15] that the steady state is achieved if

$$0 < \alpha_j < \frac{2}{\lambda_j}, \qquad \text{for } j=1,\ldots,N-1. \quad (7)$$

For $j=N$, the condition for steady state is given by

$$|\,1-\alpha_N(n)\lambda_N(n)\,| < 1 \quad (8)$$

and $\alpha_N(n)$ = **Error!**, where b is a constant. (9)

Equation (9) imposes time-varying constraint on $\alpha_N(n)$ whereas the constraints on remaining step-size parameters in the decoupled weight vector space are time-invariant as is evident from (7). The selection of step-size parameters α_i's is very critical for the LMS algorithm. Inappropriate α_i's will result in divergence from the steady state solution because one eigenvalue is increasing as a function of time index n.

The next section discusses the MSWE analysis under steady state for estimation of frequency selective randomly time-varying channels.

3 Estimation of Frequency Selective Randomly time-varying channels

In this section, we first present the system model for channel estimation and then proceed with the analytic computation of MSWE under steady state. Consider a discrete-time channel estimation model shown in Fig.2.

The desired signal $d(n)$ is an observation at the time index n that can be represented as

$$d(n) = \mathbf{w}^*(n)\mathbf{x}(n) + c(n), \quad (10)$$

where $c(n)$ denotes a zero mean Gaussian channel noise with variance σ_c^2, $\mathbf{x}(n) = [x(n)\ x(n-1)\ \ldots.\ x(n-N+1)]^{\mathrm{T}}$ represents channel input signal (or the transmitted signal) that is a discrete-time fractional Brownian motion with Hurst exponent H belonging to the range $0<H<1$, and $\mathbf{w}(n)=[w_0(n)\ w_1(n)\ldots..w_{N-1}(n)]^{\mathrm{T}}$ is the channel weight vector of length N.

From Fig.2, the LMS estimate of channel $\mathbf{w}(\cdot)$, denoted by $\hat{\mathbf{w}}(\cdot)$, at time index n is given as

$$\hat{\mathbf{w}}(n+1) = \hat{\mathbf{w}}(n) + \boldsymbol{\alpha}(n)\mathbf{x}(n)e^*(n), \quad (11)$$

where $\boldsymbol{\alpha}(n)$ is the non-diagonal step-size matrix that is simultaneously diagonalizable with the auto-covariance matrix $\mathbf{R}(n)$ of the input signal (as discussed in Section-2) and $e(n)$ denotes the estimation error at time index n and is given as

$$e(n) = d(n) - \hat{d}(n). \tag{12}$$

From Fig.2, the estimate of desired signal $\hat{d}(n)$ is given by

$$\hat{d}(n) = \hat{\mathbf{w}}^*(n)\mathbf{x}(n). \tag{13}$$

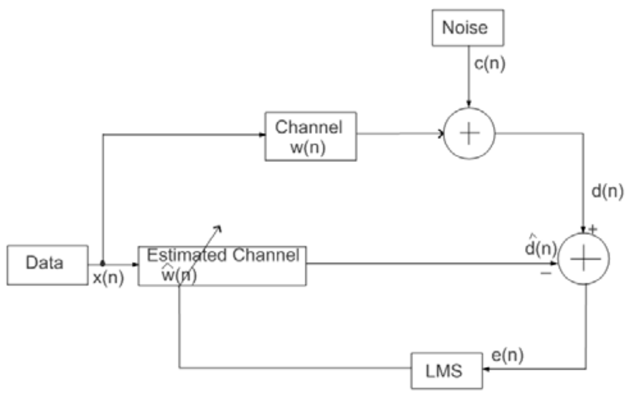

Figure-2: Channel Estimation Model

On substituting (10) and (13) in (12), we obtain

$$e(n) = \mathbf{w}^*(n)\mathbf{x}(n) + c(n) - \hat{\mathbf{w}}^*(n)\mathbf{x}(n). \tag{14}$$

Define weight error vector as $\mathbf{v}(n)$, where

$$\mathbf{v}(n) \overset{\text{def}}{=} \mathbf{w}(n) - \hat{\mathbf{w}}(n). \tag{15}$$

For the channel estimation model of Fig.2, we use one more assumption AS3 stated as below.

AS3) The sequence $\{c(\cdot)\}$ is a zero mean, white-noise stationary process, statistically independent of $\{\mathbf{x}(\cdot)\}$ and $\{\mathbf{w}(\cdot)\}$.

3.1 Computation of Analytic Expression for Mean Square Weight Error

The performance of the channel estimation model is measured with respect to the minimum mean square weight error resulting from the error between actual channel weight vector and its estimated value. In this sub-section, we aim to compute the mean squared weight error to assess the performance of FB-VSLMS algorithm in channel estimation.

Define mean squared weight error (MSWE) $D(n)$ as

$$D(n) = \mathrm{Tr}\{\mathbf{K}(n)\}, \tag{16}$$

where $\mathbf{K}(n)$ is the auto-covariance matrix of the deviation in weight vector $\mathbf{v}(n)$ and is defined as

$$\mathbf{K}(n) = \mathrm{E}[\mathbf{v}(n)\mathbf{v}^*(n)]. \tag{17}$$

On substituting (14) and (15) in (11), the weight vector updating process of the LMS algorithm is given by

$$\hat{\mathbf{w}}(n+1) = \hat{\mathbf{w}}(n) + \boldsymbol{\alpha}(n)\mathbf{x}(n)\mathbf{x}^*(n)\mathbf{v}(n) + \boldsymbol{\alpha}(n)\mathbf{x}(n)c^*(n) \tag{18}$$

It is shown in (A.28) of Appendix-A that under stationary conditions, the mean square weight error, MSWE at time index n is

$$D(n) = \frac{1}{2(1-\gamma)}\left\{J_{\mathrm{ex}}(n) + \sigma_c^2\right\}\mathrm{Tr}\left[\boldsymbol{\Lambda}_{\boldsymbol{\alpha}}(n)\right] + \sum_{k=0}^{n-1}(1-\gamma)^k \,\mathrm{Tr}\left[\mathbf{R}_{\mathbf{w}}(k+1) - \mathbf{R}_{\mathbf{w}}(k+2)\right] + \frac{1}{(1-\gamma)}\mathrm{Tr}\left[\mathbf{R}_{\mathbf{w}}(0) - \mathbf{R}_{\mathbf{w}}(1)\right], \tag{19}$$

where $J_{\mathrm{ex}}(n)$ is the excess mean square error,

$$\mathbf{R}_{\mathbf{w}}(k) = \mathrm{E}[\mathbf{w}(n)\mathbf{w}^*(n+k)]$$

and

$$\hat{\boldsymbol{\Lambda}}(n)\boldsymbol{\Lambda}_{\boldsymbol{\alpha}}(n) = \gamma\mathbf{I} \tag{20}$$

with γ as a scalar step-size parameter.

For a discrete-time Wide-sense Stationary Uncorrelated Scattering (WSSUS) channel [1, 19, 20], the discrete multipath intensity profile is given by a diagonal matrix as below:

$$\mathbf{R}_{\mathbf{w}}(\tau) = \begin{pmatrix} R_0(\tau)\rho_0^2 & 0 & . & . & 0 \\ 0 & R_1(\tau)\rho_1^2 & 0 & . & . \\ . & 0 & . & . & . \\ . & . & . & . & 0 \\ 0 & . & . & 0 & R_{L-1}(\tau)\rho_{L-1}^2 \end{pmatrix}. \tag{21a}$$

Assuming that the channel coefficients have the same auto-correlation function $R(\tau)$

$$\mathrm{Tr}[\mathbf{R}_{\mathrm{w}}(\tau)] = \sigma_{\mathrm{w}}^2 R(\tau), \tag{21b}$$

where $\sigma_{\mathbf{w}}^2 = \rho_0^2 + ... + \rho_{L-1}^2$ is the channel gain (for normalized channel σ_w^2=1).

On substituting (21b) in (19), we obtain

$$D(n) = \frac{1}{2(1-\gamma)}\left\{J_{\mathrm{ex}}(n) + \sigma_c^2\right\}\mathrm{Tr}\left[\boldsymbol{\Lambda}_{\boldsymbol{\alpha}}(n)\right] + \sum_{k=0}^{n-1}(1-\gamma)^k \sigma_{\mathbf{w}}^2\left[R(k+1) - R(k+2)\right] + \frac{1}{(1-\gamma)}\sigma_{\mathbf{w}}^2\left[R(0) - R(1)\right]. \tag{22}$$

In the following subsection, we compute the analytic expression for optimum step-size parameter for two channel models. Because the use of MSE and MSWE is equivalent for step-size optimization [4], we focus only on MSWE to evaluate the performance of the proposed approach of channel estimation.

3.2 Mean Square Weight Error and Optimum FB-LMS Step-Size Parameter for Frequency Selective Time-Varying Channels

In this subsection, we analyze MSWE for two channel models, namely, the class of asymptotically stationary AR processes [3-4, 20-21] and the Jakes model [19-20, 22-23]. These channels are important because small-scale fading Rayleigh channels are generally characterized by these channel models. The Jakes model and AR process channel model are examples of Gaussian WSSUS channel where each tap is uncorrelated. The individual taps are modeled with Rayleigh distributed amplitude and uniformly distributed phase between $-\pi$ to π.

First, let us consider the class of asymptotically stationary AR channel model. For an AR process channel, taps are generated via an AR process and have spectrum shape defined by Doppler spread profile [3].

3.2.1 Asymptotically Stationary AR Process Channel Model

The autocorrelation function associated with an asymptotically AR process of order M, after its transient period, can be expressed as [21]

$$\sum_{i=0}^{M} a_i R(l-i) = 0\,, \qquad l \geq 0 \tag{23}$$

and $$R(k) = \sum_{i=1}^{M} c_i\, p_i^k\,, \tag{24}$$

where a_i's are AR parameters with a_0=1, c_i's are constants, and p_i's are roots of the coefficient equation

$$1 + a_1 z^{-1} + a_2 z^{-2} + ...a_M z^{-M} = 0\,. \tag{25}$$

It is to note that for asymptotic stationarity of an AR process $|p_i|<1$ for all i and because step-size parameter (γ) is also small in applications of wireless communications [4], we assume

$$|(1-\gamma)\, p_i| < 1 \qquad \text{for all } i. \tag{26}$$

Because we know that $\hat{\mathbf{\Lambda}}(n)\mathbf{\Lambda}_{\boldsymbol{\alpha}}(n) = \gamma\mathbf{I}\,,$ (27)

$$\mathrm{Tr}\left[\mathbf{\Lambda}_{\boldsymbol{\alpha}}(n)\right] = \mathrm{Tr}\begin{pmatrix} \frac{\gamma}{\lambda_1} & 0 & . & . & 0 \\ 0 & \frac{\gamma}{\lambda_2} & . & . & 0 \\ . & 0 & . & . & . \\ 0 & . & . & \frac{\gamma}{\lambda_{N\text{-}1}} & 0 \\ 0 & . & . & . & \frac{\gamma}{\lambda_N(n)} \end{pmatrix}. \tag{28}$$

The expression in (28) simplifies as below:

$$\mathrm{Tr}\left[\mathbf{\Lambda}_{\boldsymbol{\alpha}}(n)\right] = \gamma \sum_{i=1}^{N} \frac{1}{\lambda_i}\,, \tag{29}$$

with the largest eigenvalues $\lambda_N(n) \to \infty$ and hence, $1/\lambda_N(n) \to 0$.

On substituting (24) in (22), and using (26), (28), and (29), we obtain MSWE as given below [24]:

$$D(n) = \frac{\gamma\left\{J_{\mathrm{ex}}(n) + \sigma_c^2\right\}}{2(1-\gamma)} \sum_{i=1}^{N} \frac{1}{\lambda_i} + \sum_{i=1}^{M} \frac{\sigma_{\mathbf{w}}^2 c_i (1-p_i)}{(1-\gamma) - (1-\gamma)^2 p_i}\,. \tag{30}$$

where $J_{\mathrm{ex}}(n) = \mathrm{Tr}\left[\mathbf{K}(n)\mathbf{R}(n)\right]$.

The average excess mean square error can be easily shown to be bounded between [21]

$$\lambda_{\min} D(n) \leq J_{\mathrm{ex}}(n) \leq \lambda_{\max} D(n) \tag{31}$$

On considering the worst case condition for $J_{\mathrm{ex}}(n)$ and using the upper bound $\lambda_{\max} D(n)$ of (31) in (30), we obtain

$$\left(1 - \frac{\gamma\lambda_{\max}}{2(1-\gamma)} \sum_{i=1}^{N} \frac{1}{\lambda_i}\right) D(n) = \frac{\gamma\sigma_c^2}{2(1-\gamma)} \sum_{i=1}^{N} \frac{1}{\lambda_i} + \sum_{i=1}^{M} \frac{\sigma_{\mathbf{w}}^2 c_i (1-p_i)}{(1-\gamma) - (1-\gamma)^2 p_i} \tag{32}$$

As time index n increases, $\lambda_{\max} \sum_{i=1}^{N} \frac{1}{\lambda_i} \to 1$ and therefore (32) can be rewritten as

$$D(n,\gamma) \overset{def}{=} D(n) = \frac{1}{A} \frac{\gamma\sigma_c^2}{2(1-\gamma)} \sum_{i=1}^{N} \frac{1}{\lambda_i} + \frac{1}{A} \sum_{i=1}^{M} \frac{\sigma_{\mathbf{w}}^2 c_i (1-p_i)}{(1-\gamma) - (1-\gamma)^2 p_i} \tag{33}$$

where $A = \left(1 - \frac{\gamma}{2(1-\gamma)}\right)$ = constant dependent on γ. (34)

Because A has to be positive, this puts a constraint on γ as below

$$0 < \gamma < \frac{2}{3} \tag{35}$$

In the steady state as $n \to \infty$, $\lambda_N(n) \to \infty$ and hence, $1/\lambda_N(n) \to 0$. Thus, MSWE becomes independent of time index n and is only a function of γ. Therefore, in the steady state, we can rewrite MSWE $D(n,\gamma)$ using (33) and (34) as below:

$$D(\gamma) = \frac{\gamma\sigma_c^2}{(2-3\gamma)}\sum_{i=1}^{N-1}\frac{1}{\lambda_i} + \frac{2}{(2-3\gamma)}\sum_{i=1}^{M}\frac{\sigma_{\mathrm{w}}^2 c_i(1-p_i)}{1-(1-\gamma)p_i} \tag{36}$$

From (36), for an AR process of order-1, MSWE in the steady state is given by

$$D(\gamma) = \frac{\gamma\sigma_c^2}{(2-3\gamma)}\sum_{i=1}^{N-1}\frac{1}{\lambda_i} + \frac{2\sigma_{\mathrm{w}}^2 c_1(1-p_1)}{(2-3\gamma)(1-(1-\gamma)p_1)} \tag{37}$$

To minimize $D(\gamma)$, we differentiate $D(\gamma)$ in (37) with respect to the step-size parameter (γ) and equate it to zero. Thus, for a channel characterized by an asymptotically stationary AR process of order-1, we find the optimum step-size parameter (γ^*) in (38).

$$\gamma^* = \left(1-\frac{1}{p_1}\right) - \frac{3}{p_1}.\frac{\sigma_{\mathrm{w}}^2 c_1(1-p_1)}{\sigma_c^2\sum_{i=1}^{N-1}\frac{1}{\lambda_i}} + \frac{3}{p_1}.\sqrt{\left(\frac{\sigma_{\mathrm{w}}^2 c_1(1-p_1)}{\sigma_c^2\sum_{i=1}^{N-1}\frac{1}{\lambda_i}}\right)^2 + \frac{2\sigma_{\mathrm{w}}^2 c_1(1-p_1)(5-3p_1)}{9\sigma_c^2\sum_{i=1}^{N-1}\frac{1}{\lambda_i}}} \tag{38}$$

Similarly, for a channel characterized by an asymptotically stationary AR process of order-2, MSWE in the steady state is given by

$$D(\gamma) = \frac{\gamma\sigma_c^2}{(2-3\gamma)}\sum_{i=1}^{N-1}\frac{1}{\lambda_i} + \sum_{i=1}^{2}\frac{2\sigma_{\mathrm{w}}^2 c_i(1-p_i)}{(2-3\gamma)[1-(1-\gamma)p_i]}. \tag{39}$$

On differentiating $D(\gamma)$ in (39) with respect to the step-size parameter (γ) and equating it to zero, we obtain

$$A_0 + A_1\gamma + A_2\gamma^2 + A_3\gamma^3 + A_4\gamma^4 = 0, \tag{40}$$

where, A_i's are constants and γ_i's are the solutions of (40).

Therefore, the optimum step-size (γ^*) is given by

$$\gamma^* = \min\{D(\gamma_1), D(\gamma_2), D(\gamma_3), D(\gamma_4)\}. \tag{41}$$

3.2.2 Jakes Channel Model

For the Jakes channel model, the autocorrelation function is given by [22-23, 25]

$$R(k) = J_0(2\pi f_D T k) \tag{42}$$

where $J_0(\cdot)$ is the zero-order Bessel function of the first kind, $f_D = \frac{v}{\lambda_c}$ is the maximum Doppler shift, v is the mobile speed, λ_c is the carrier wavelength, and T is the sample interval. On substituting (42) in (22), we obtain

$$D(n) = \frac{1}{2(1-\gamma)}\left\{J_{\mathrm{ex}}(n) + \sigma_c^2\right\}\mathrm{Tr}[\mathbf{\Lambda}_{\boldsymbol{\alpha}}(n)] + \sum_{k=0}^{n-1}(1-\gamma)^k\sigma_{\mathbf{w}}^2[J_0(2\pi f_D T(k+1)) - J_0(2\pi f_D T(k+2))] + \frac{1}{(1-\gamma)}\sigma_{\mathbf{w}}^2[J_0(0) - J_0(2\pi f_D T)]. \tag{43}$$

In the steady state (43) reduces to (44) as shown below.

$$D(\gamma) = \frac{\gamma\sigma_c^2}{(2-3\gamma)}\sum_{i=1}^{N-1}\frac{1}{\lambda_i} + \frac{2}{2-3\gamma}\sum_{k=0}^{\infty}(1-\gamma)^{k-1}\sigma_{\mathrm{w}}^2[J_0(2\pi f_D T(k+1)) - J_0(2\pi f_D T(k+2))] + \frac{2}{(2-3\gamma)}\sigma_{\mathrm{w}}^2[J_0(0) - J_0(2\pi f_D T)]. \tag{44}$$

Because a good analytical approximation of the Jakes model can be obtained with an AR process [3], we use the same technique as suggested in [4] to compute the optimum step-size parameter for Jakes channel model. Therefore, optimum parameters for a Jakes channel modeled as an AR process of order M are given by (45).

$$\mathbf{a} = \mathbf{R}_J^{-1} r_J(1), \tag{45}$$

where

$$\mathbf{R}_J = \begin{pmatrix} 1 & J_0(\tau) & \ldots & J_0(\tau(M-1)) \\ J_0(\tau) & 1 & \cdots & J_0(\tau(M-2)) \\ \vdots & \vdots & \vdots & \vdots \\ J_0(\tau(M-1)) & \cdots & J_0(\tau) & 1 \end{pmatrix},$$

$$r_J(m) = \left(J_0(\tau m) \quad \cdots \quad J_0(\tau(m+M-1))\right)^{\mathrm{T}},$$

and $\tau = 2\pi f_D T$. From the parameter vector $\boldsymbol{a}$, we can estimate p_i's by solving (25), and hence estimate c_i's using (46) given as below:

$$\mathbf{c} = \mathbf{P}^{-1} r_J(0), \tag{46}$$

where $$\mathbf{P} = \begin{pmatrix} 1 & 1 & \ldots & 1 \\ p_1 & p_2 & \cdots & p_M \\ \vdots & \vdots & \vdots & \vdots \\ p_1^{M-1} & p_2^{M-1} & \ldots & p_M^{M-1} \end{pmatrix}.$$

For a Jakes channel modeled using AR-2 system, the optimum step-size (γ^*) can be calculated by differentiating $D(\gamma)$ in (44) with respect to the step-size parameter (γ) and using (40), and (41) as discussed in the previous subsection.

In the next section, we present simulation results on the above discussed channels. We present the comparison of analytical and the simulated results of MSWE as a function of scalar step-size parameter (γ). We also compare the analytical result of optimum step-size parameter (γ^*) with the estimated simulation results.

4 Simulation Results

In this section, we present some simulation results to validate the theory developed in section 3 above. We compare our analytical results of MSWE vs γ with the analytical results presented in [4]. All experiments are conducted assuming that first 20% samples of a block of samples are available at the receiver as the training samples for channel estimation. The channel coefficients do not vary over one block (a slow fading channel) and the channel is estimated during the training period using the training sample data.

4.1 Simulation results on Asymptotically Stationary AR Process Channel Model

In the first experimental set-up, we consider two tap channel model, i.e., N=no. of channel taps =2. Channel weights at each iteration are produced by feeding zero mean complex white Gaussian noise of variance σ_g^2 as input to an AR-1 system with parameter a_1= -0.99. The parameter a_1 lies between -0.9 to -0.999 for a wireless channel [3-4, 6]. The channel SNR is considered to be variable between 5dB to 20 dB (by choosing appropriate value of σ_c^2), σ_w^2 =1 (normalized channel with unity channel power gain), and a non-stationary input signal with varying value of H as input to the channel. Table-1 displays parameter values for the experimental set-up.

Fig. 3 displays MSWE vs γ over asymptotically stationary AR-1 channel for analytical versus simulation results. Simulations are carried out over 50 sample functions of noise, 25 sample functions of channel with 8000 time iterations (n) for each sample function. It is observed that the MSWE achieved via simulation is lower than that achieved with the analytical results. This is due to the fact that we considered worst (or the upper bound of) excess mean squared error from (31) in the analytical results. Thus, our analytical results are conservative leading to better simulation results compared to the analytical results.

Fig. 4 displays analytical results of MSWE vs γ over asymptotically stationary AR-1 channel with varying variance σ_g^2 that is used to generate channel weights. It is observed that the performance of the proposed approach is better than [4] until σ_g^2 increases beyond 0.1.

Table 1: Parameter values for the experimental set-up-1

Parameters	Fig. 3	Fig. 4	Fig. 5	Fig. 6
N=no. of channel taps	2	2	2	2
a_1 (AR 1 channel coefficient)	-0.99	-0.99	-0.99	-0.99
Variance (σ_g^2)of complex WGN used to generate channel weights	0.01	Variable	0.01	0.01
H (Hurst exponent of input signal)	Variable	0.1	0.1	0.1
Channel SNR	10dB	10dB	Variable	Variable
Block length	80	80	80	80
No. of training samples in a block	16	16	16	16

Fig. 5 displays MSWE vs γ over asymptotically stationary AR-1 channel with varying channel SNR. We observe that the performance of the proposed approach is better than [4] at lower SNR (at 5 dB and 10 dB), while at 20dB SNR, [4] perform slightly better than the proposed approach.

From Fig. 6, we observe that the minimum mean squared weight error is achieved with the lowest value of H and as the value of H increases, the MSWE curve shifts upwards. This is obvious because as the value of H increases, the correlation in the input signal increases, while the LMS algorithm performs best when the input signal is uncorrelated. The performance of the FB-VSLMS algorithm is better than [4], until H increases beyond 0.25.

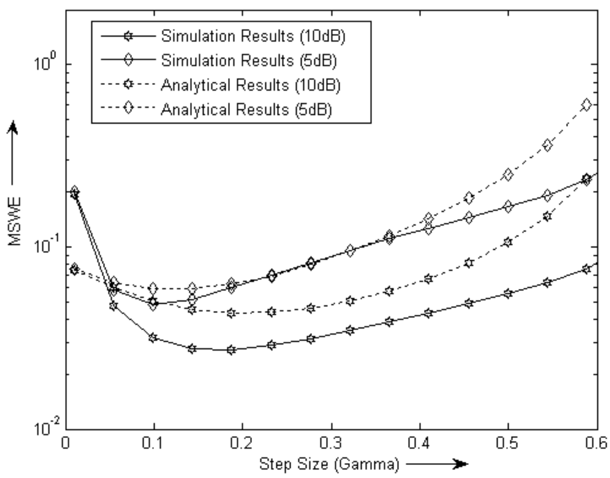

Figure-3:MSWE vs γ over an asymptotically stationary AR-1 channel: Simulation versus analytical results for the proposed approach

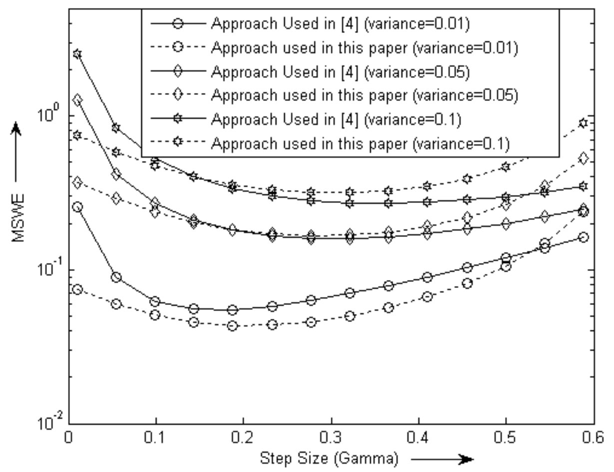

Figure-4: MSWE vs γ over an asymptotically stationary AR-1 channel with varying variance σ_g^2 that is used to generate channel weights

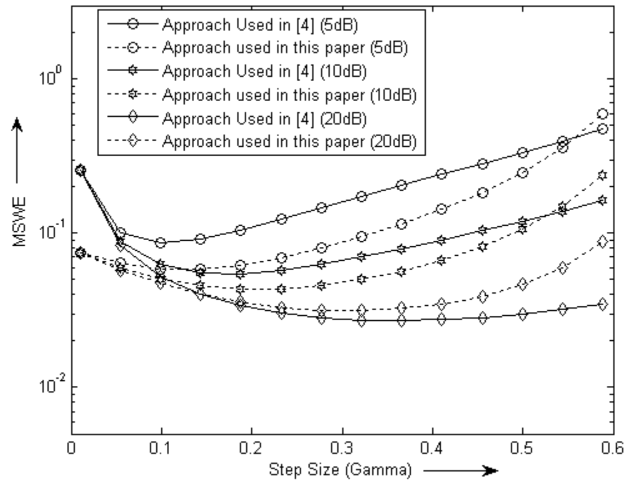

Figure-5: MSWE vs γ over an asymptotically stationary AR-1 channel with varying channel SNR

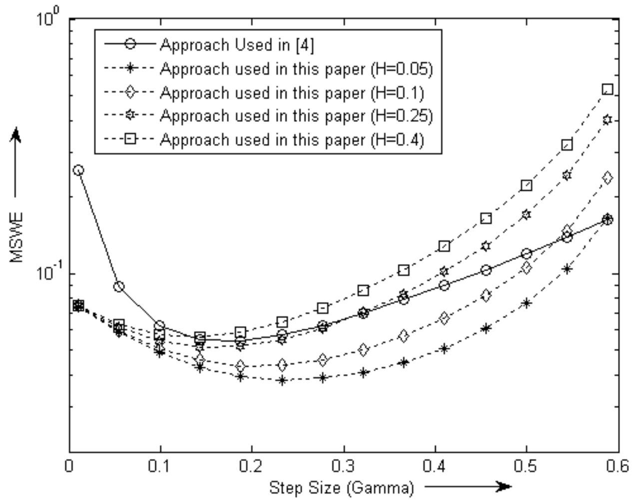

Figure-6: MSWE vs γ over an asymptotically stationary AR-1 channel with nonstationary input signal of varying H

From the above, it can be noted that our conservative analytical results are better or comparable to [4] under different scenarios. Also, from Table-2, it is observed that the optimum value of step-size parameter (γ^*) from simulation matches with the analytical results obtained using (38).

Table 2: Analytical vs Simulation values of optimum step-size (γ^*)

Parameters	γ^* calculated from (38)	γ^* estimated via simulations
H=0.1, channel SNR=5dB, σ_g^2=0.01	0.15	0.11
H=0.1, channel SNR=10dB, σ_g^2=0.01	0.22	0.19
H=0.1, channel SNR=20dB, σ_g^2=0.01	0.31	0.33

4.2 Simulation results on Jakes Channel Model

In the second experimental set-up, we consider three tap (N=no. of channel taps =3) Jakes channel. For the Jakes Doppler spectrum, two values of f_DT (0.005 and 0.01) are considered. The channel SNR is considered to be variable between 5dB to 20 dB (by choosing appropriate value of σ_c^2), σ_w^2 =1 (normalized channel with unity channel power gain), and a non-stationary input signal with varying value of H as input to the channel. Table-3 displays parameter values for the experimental set-up. In [3], it has been shown that a good analytical approximation of the Jakes model can be obtained with an AR process of order 2, we have considered AR-2 system model for modeling Jakes spectrum and used (45) and (46) to estimate system coefficients (a_i's).

Table 3: Parameter values for the experimental set-up- 2

Parameters	**Fig. 7**	**Fig. 8**	**Fig. 9**	**Fig. 10**
N=no. of channel taps	3	3	3	3
f_DT	Variable	0.005	Variable	0.005
H (Hurst exponent of input signal)	0.1	Variable	0.1	0.1
Channel SNR	10dB	10dB	10dB	Variable
Block length	100	100	100	100
No. of training samples in a block	20	20	20	20

Fig. 7 displays MSWE vs γ over Jakes channel for analytical versus simulation results for two values of f_DT (0.005 and 0.01). Simulations are carried out over 50 sample functions of noise, 25 sample functions of channel with 8000 time iterations (n) for each sample function. It is observed that MSWE decreases as the value of f_DT decreases where f_DT is a measure of speed of the vehicle. This is obvious because as the mobile moves with a higher speed, the tracking performance degrades. Again, we notice that the simulation results are better than the analytical results because the upper bound of averaged excess mean squared error (J_{ex}) is used in the analytical computation of MSWE and that would be higher than the actual value of J_{ex} in simulations.

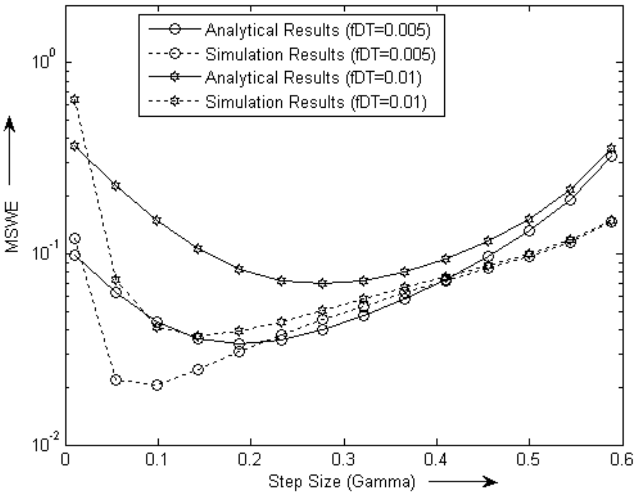

Figure-7: MSWE vs γ over Jakes channel with varying $f_D T$: Simulation versus analytical results for the proposed approach

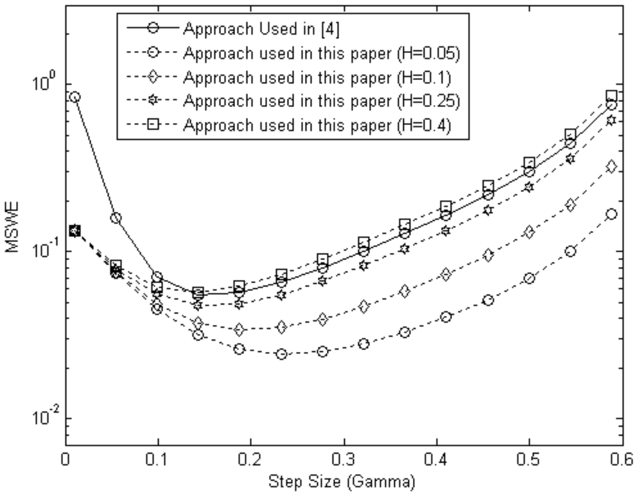

Figure-8: MSWE vs γ over Jakes channel with nonstationary input signal of varying H

Figures 8 to 10 present the comparative performance of [4] and the proposed approach for the analytical results of MSWE vs γ. It should be noted that the comparison is presented for the conservative results of the proposed approach as explained above. From Fig. 8, we observe that the MSWE curve shifts upwards as the value of H increases because the correlation in the input signal increases. Fig. 9 displays MSWE vs γ for two values of $f_D T$. Fig. 10 displays MSWE vs γ over Jakes channel for varying channel SNR. From these figures, we observe that the performance of the proposed approach is better than [4] under different scenarios .Also, as the channel SNR decreases, comparative performance of the proposed approach improves further.

Thus, we observe that the proposed approach is able to estimate multipath fading channel efficiently when nonstationary signal is transmitted over the channel.

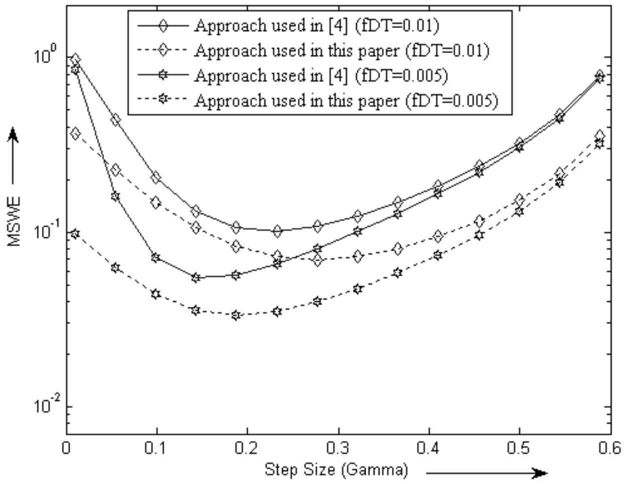

Figure-9: MSWE vs γ over Jakes channel with varying $f_D T$: Comparison of analytical results of [4] with the proposed approach

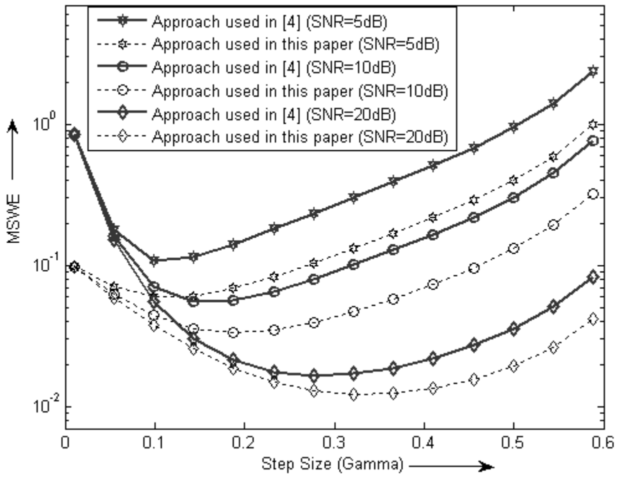

Figure-10: MSWE vs γ over Jakes channel for varying channel SNR: Comparison of analytical results of [4] with the proposed approach

5 Conclusions

In this paper, we have evaluated the performance of the fBm based variable step-size LMS (FB-VSLMS) algorithm on the estimation of multipath fading channel for the transmission of a class of nonstationary process. We considered asymptotically stationary AR channels and Jakes channel that are examples of Gaussian WSSUS channel model. The algorithm exploits the statistics of the non-stationary process to design an adaptive LMS filter in order to estimate these channels. We derived the analytical expressions of steady-state mean-square weight error (MSWE) and the optimum step-size parameter. Thus, instead of estimating the optimum step-size during simulations, analytical expression can be used for the same to estimate the channel reliably in real time. Simulation results show that the FB-VSLMS algorithm is indeed effective in estimating such randomly time-varying channels.

Appendix-A

Calculation of MSWE

From (15), weight error vector at time index n +1 is

$$\mathbf{v}(n+1) = \mathbf{w}(n+1) - \hat{\mathbf{w}}(n+1) \tag{A.1}$$

Define a-priori weight vector error $\mathbf{v}_\mathrm{p}(n)$ as

$$\mathbf{v}_\mathrm{p}(n) \overset{\mathrm{def}}{=} \mathbf{w}(n+1) - \hat{\mathbf{w}}(n)\,. \tag{A.2}$$

On substituting (18) and (A.2) in (A.1), we obtain

$$\begin{aligned}\mathbf{v}(n+1) &= \mathbf{w}(n+1) - \hat{\mathbf{w}}(n) - \boldsymbol{\alpha}(n)\mathbf{x}(n)\mathbf{x}^*(n)\mathbf{v}(n) \\ &\quad - \boldsymbol{\alpha}(n)\mathbf{x}(n)c^*(n) \\ &= \mathbf{v}_\mathrm{p}(n) - \boldsymbol{\alpha}(n)\mathbf{x}(n)\mathbf{x}^*(n)\mathbf{v}(n) - \boldsymbol{\alpha}(n)\mathbf{x}(n)c^*(n)\end{aligned} \tag{A.3}$$

We use (A.3) to evaluate the auto-covariance matrix of the deviation in weight vector, $\mathbf{v}(n)$, at time index n+1 as

$$\begin{aligned}\mathbf{K}(n+1) &= E\left[\mathbf{v}(n+1)\mathbf{v}^*(n+1)\right] \\ &= E\left[\mathbf{v}_\mathrm{p}(n)\mathbf{v}_\mathrm{p}^*(n)\right] - E\left[\mathbf{v}_\mathrm{p}(n)\mathbf{v}^*(n)\mathbf{x}(n)\mathbf{x}^*(n)\boldsymbol{\alpha}(n)\right] \\ &- E\left[\mathbf{v}_\mathrm{p}(n)\mathbf{x}^*(n)\boldsymbol{\alpha}(n)c(n)\right] \\ &- E\left[\boldsymbol{\alpha}(n)\mathbf{x}(n)\mathbf{x}^*(n)\mathbf{v}(n)\mathbf{v}_\mathrm{p}^*(n)\right] \\ &- E\left[\boldsymbol{\alpha}(n)\mathbf{x}(n)\mathbf{x}^*(n)\mathbf{v}(n)\mathbf{v}^*(n)\mathbf{x}(n)\mathbf{x}^*(n)\boldsymbol{\alpha}(n)\right] \\ &- E\left[\boldsymbol{\alpha}(n)\mathbf{x}(n)\mathbf{x}^*(n)\mathbf{v}(n)\mathbf{x}^*(n)\boldsymbol{\alpha}(n)c(n)\right] \\ &- E\left[\boldsymbol{\alpha}(n)\mathbf{x}(n)\mathbf{v}_\mathrm{p}^*(n)c^*(n)\right] \\ &- E\left[\boldsymbol{\alpha}(n)\mathbf{x}(n)\mathbf{v}^*(n)\mathbf{x}(n)\mathbf{x}^*(n)\boldsymbol{\alpha}(n)c^*(n)\right] \\ &- E\left[\boldsymbol{\alpha}(n)\mathbf{x}(n)\mathbf{x}^*(n)\boldsymbol{\alpha}(n)\left|c(n)\right|^2\right].\end{aligned} \tag{A.4}$$

Using assumption AS2 and AS3, we can conclude that $\mathbf{v}(n)$, $\mathbf{x}(n)$ and $c(n)$ are statistically independent. This further implies that $\mathbf{v}_\mathrm{p}(n)$, $\mathbf{x}(n)$ and $c(n)$ are also statistically independent of each other. Thus, we can simplify (A.4) as

$$\begin{aligned}\mathbf{K}(n+1) &= \mathbf{K}_\mathrm{p}(n) - \tilde{\mathbf{K}}_\mathrm{p}(n)\mathbf{R}(n)\boldsymbol{\alpha}(n) - \boldsymbol{\alpha}(n)\mathbf{R}(n)\tilde{\mathbf{K}}_\mathrm{p}(n) \\ &+ \boldsymbol{\alpha}(n)E\left[\mathbf{x}(n)\mathbf{x}^*(n)\mathbf{v}(n)\mathbf{v}^*(n)\mathbf{x}(n)\mathbf{x}^*(n)\right]\boldsymbol{\alpha}(n) \\ &\quad + \boldsymbol{\alpha}(n)\mathbf{R}(n)\boldsymbol{\alpha}(n)\sigma_c^2\end{aligned} \tag{A.5a}$$

where $\mathbf{K}_\mathrm{p}(n) \overset{\mathrm{def}}{=} E\left[\mathbf{v}_\mathrm{p}(n)\mathbf{v}_\mathrm{p}^*(n)\right],$ (A.5b)

$$\tilde{\mathbf{K}}_\mathrm{p}(n) \overset{\mathrm{def}}{=} E\left[\mathbf{v}_\mathrm{p}(n)\mathbf{v}^*(n)\right], \tag{A.5c}$$

and $\mathbf{R}(n) \overset{\mathrm{def}}{=} E\left[\mathbf{x}(n)\mathbf{x}^*(n)\right].$ (A.5d)

It can be easily shown that

$$\begin{aligned}&E\left[\mathbf{x}(n)\mathbf{x}^*(n)\mathbf{v}(n)\mathbf{v}^*(n)\mathbf{x}(n)\mathbf{x}^*(n)\right] \\ &= 2\mathbf{R}(n)\mathbf{K}(n)\mathbf{R}(n) + \mathbf{R}(n)\mathrm{Tr}\left[\mathbf{R}(n)\mathbf{K}(n)\right].\end{aligned} \tag{A.6}$$

Therefore, on substituting (A.6) in (A.4), we get

$$\begin{aligned}\mathbf{K}(n+1) &= \mathbf{K}_\mathrm{p}(n) - \tilde{\mathbf{K}}_\mathrm{p}(n)\mathbf{R}(n)\boldsymbol{\alpha}(n) - \boldsymbol{\alpha}(n)\mathbf{R}(n)\tilde{\mathbf{K}}_\mathrm{p}(n) \\ &+ 2\boldsymbol{\alpha}(n)\mathbf{R}(n)\mathbf{K}(n)\mathbf{R}(n)\boldsymbol{\alpha}(n) \\ &+ \boldsymbol{\alpha}(n)\mathbf{R}(n)\boldsymbol{\alpha}(n)\mathrm{Tr}\left[\mathbf{R}(n)\mathbf{K}(n)\right] + \boldsymbol{\alpha}(n)\mathbf{R}(n)\boldsymbol{\alpha}(n)\sigma_c^2\,.\end{aligned} \tag{A.7}$$

To simplify (A.7), define excess mean square error, $J_\mathrm{ex}(n)$ as

$$J_\mathrm{ex}(n) = \mathrm{Tr}\left[\mathbf{R}(n)\mathbf{K}(n)\right]. \tag{A.8}$$

On substituting (A.8) in (A.7), we obtain

$$\begin{aligned}\mathbf{K}(n+1) &= \mathbf{K}_\mathrm{p}(n) - \tilde{\mathbf{K}}_\mathrm{p}(n)\mathbf{R}(n)\boldsymbol{\alpha}(n) - \boldsymbol{\alpha}(n)\mathbf{R}(n)\tilde{\mathbf{K}}_\mathrm{p}(n) \\ &+ 2\boldsymbol{\alpha}(n)\mathbf{R}(n)\mathbf{K}(n)\mathbf{R}(n)\boldsymbol{\alpha}(n) + \boldsymbol{\alpha}(n)\mathbf{R}(n)\boldsymbol{\alpha}(n)J_\mathrm{ex}(n) \\ &+ \boldsymbol{\alpha}(n)\mathbf{R}(n)\boldsymbol{\alpha}(n)\sigma_c^2\,.\end{aligned} \tag{A.9}$$

We use (A.9) to compute the analytic expression of MSWE $D(\cdot)$, at time index n+1, as

$$\begin{aligned}D(n+1) &= \mathrm{Tr}\left[\mathbf{K}(n+1)\right] \\ &= \mathrm{Tr}\left[\mathbf{K}_\mathrm{p}(n)\right] - \mathrm{Tr}\left[\tilde{\mathbf{K}}_\mathrm{p}(n)\mathbf{R}(n)\boldsymbol{\alpha}(n)\right] - \mathrm{Tr}\left[\boldsymbol{\alpha}(n)\mathbf{R}(n)\tilde{\mathbf{K}}_\mathrm{p}(n)\right] \\ &\quad + 2\mathrm{Tr}\left[\boldsymbol{\alpha}(n)\mathbf{R}(n)\mathbf{K}(n)\mathbf{R}(n)\boldsymbol{\alpha}(n)\right] \\ &\quad + \mathrm{Tr}\left[\boldsymbol{\alpha}(n)\mathbf{R}(n)\boldsymbol{\alpha}(n)\right]\left\{J_\mathrm{ex}(n) + \sigma_c^2\right\}.\end{aligned} \tag{A.10}$$

From Theorem-1, we know that $\mathbf{R}(n)$ can be approximated as $\hat{\mathbf{R}}(n)$ for large n such that

$$\hat{\mathbf{R}}(n) = \mathbf{Q}\hat{\boldsymbol{\Lambda}}(n)\mathbf{Q}^\mathrm{T}, \tag{A.11}$$

We use assumption AS1, (2), and (A.11) for large n to simplify (A.10) and obtain

$$\begin{aligned}D(n+1) &= \mathrm{Tr}\left[\mathbf{K}_\mathrm{p}(n)\right] - 2\mathrm{Tr}\left[\tilde{\mathbf{K}}_\mathrm{p}(n)\mathbf{Q}\hat{\boldsymbol{\Lambda}}(n)\boldsymbol{\Lambda}_{\boldsymbol{\alpha}}(n)\mathbf{Q}^\mathrm{T}\right] \\ &\quad + 2\mathrm{Tr}\left[\mathbf{R}(n)\boldsymbol{\alpha}(n)\boldsymbol{\alpha}(n)\mathbf{R}(n)\mathbf{K}(n)\right] \\ &\quad + \mathrm{Tr}\left[\mathbf{Q}\boldsymbol{\Lambda}_{\boldsymbol{\alpha}}(n)\hat{\boldsymbol{\Lambda}}(n)\boldsymbol{\Lambda}_{\boldsymbol{\alpha}}(n)\mathbf{Q}^\mathrm{T}\right]\left\{J_\mathrm{ex}(n) + \sigma_c^2\right\}.\end{aligned} \tag{A.12}$$

Because the diagonal matrix $\boldsymbol{\Lambda}_\alpha(n)$ defines the step-size parameters to be used with different weights in this transformed space and transforms to $\boldsymbol{\alpha}(n)$ in the original filter weight co-ordinate space using $\mathbf{Q}$ in (2), we can write

$$\hat{\boldsymbol{\Lambda}}(n)\boldsymbol{\Lambda}_{\boldsymbol{\alpha}}(n) = \gamma\mathbf{I}\,, \tag{A.13}$$

where γ is a scalar step-size parameter.

On substituting (A.13) in (A.12), we obtain

$$D(n+1) = \mathrm{Tr}\left[\mathbf{K}_p(n)\right] - 2\gamma \mathrm{Tr}\left[\tilde{\mathbf{K}}_p(n)\right] + 2\gamma^2 \mathrm{Tr}\left[\mathbf{K}(n)\right] + \gamma \mathrm{Tr}\left[\mathbf{\Lambda}_{\boldsymbol{\alpha}}(n)\right]\left\{J_{ex}(n) + \sigma_c^2\right\}. \tag{A.14}$$

In steady state, we can assume that

$$D(n+1) = D(n) \tag{A.15}$$

On substituting (A.15) in (A.14), we obtain

$$\left(1-\gamma^2\right)D(n) = \mathrm{Tr}\left[\mathbf{K}_p(n)\right] - 2\gamma \mathrm{Tr}\left[\tilde{\mathbf{K}}_p(n)\right] + \gamma \mathrm{Tr}\left[\mathbf{\Lambda}_{\boldsymbol{\alpha}}(n)\right]\left\{J_{ex}(n) + \sigma_c^2\right\} \tag{A.16}$$

To simplify (A.16), we compute the terms on the R.H.S. of (A.16).

$$\begin{aligned}\mathbf{K}_p(n) &= E\left[\mathbf{v}_p(n)\mathbf{v}_p^*(n)\right] \\ &= E\left[\left(\mathbf{w}(n+1) - \hat{\mathbf{w}}(n)\right)\left(\mathbf{w}^*(n+1) - \hat{\mathbf{w}}^*(n)\right)\right] \\ &= E\left[\left(\mathbf{w}(n+1) - \mathbf{w}(n) + \mathbf{v}(n)\right)\left(\mathbf{w}^*(n+1) - \hat{\mathbf{w}}^*(n) + \mathbf{v}^*(n)\right)\right] \\ &= E\left[\left(\mathbf{w}(n+1) - \mathbf{w}(n)\right)\mathbf{v}^*(n)\right] + E\left[\mathbf{v}(n)\left(\mathbf{w}^*(n+1) - \hat{\mathbf{w}}^*(n)\right)\right] \\ &\quad + \mathbf{K}(n) + 2\left[\mathbf{R}_w(0) - \mathbf{R}_w(1)\right]\end{aligned} \tag{A.17}$$

To simplify (A.17), consider the terms on the R.H.S. of (A.17).

$$\begin{aligned}\mathbf{\Gamma} &= E\left[\left(\mathbf{w}(n+1) - \mathbf{w}(n)\right)\mathbf{v}^*(n)\right] \\ &= E\left[\left(\mathbf{w}(n+1) - \mathbf{w}(n)\right)\left(\mathbf{w}^*(n) - \hat{\mathbf{w}}^*(n)\right)\right] \\ &= E\left[\mathbf{w}(n+1)\mathbf{w}^*(n)\right] - E\left[\mathbf{w}(n+1)\hat{\mathbf{w}}^*(n)\right] \\ &\quad - E\left[\mathbf{w}(n)\mathbf{w}^*(n)\right] + E\left[\mathbf{w}(n)\hat{\mathbf{w}}^*(n)\right] \\ &= \left[\mathbf{R}_{\mathbf{w}}(1) - \mathbf{R}_{\mathbf{w}}(0)\right] - E\left[\mathbf{w}(n+1)\hat{\mathbf{w}}^*(n)\right] \\ &\quad + E\left[\mathbf{w}(n)\hat{\mathbf{w}}^*(n)\right]\end{aligned} \tag{A.18}$$

Consider

$$\begin{aligned}E\left[\mathbf{w}(n+1)\hat{\mathbf{w}}^*(n)\right] &= E\{\mathbf{w}(n+1)[\hat{\mathbf{w}}^*(n-1) \\ &\quad + \mathbf{x}^*(n-1)\boldsymbol{\alpha}(n-1)e(n-1)]\} \\ &= E\left[\mathbf{w}(n+1)\hat{\mathbf{w}}^*(n-1)\right] \\ &\quad + E\left[\mathbf{w}(n+1)\mathbf{w}^*(n-1)\mathbf{x}(n-1)\mathbf{x}^*(n-1)\boldsymbol{\alpha}(n-1)\right] \\ &\quad - E\left[\mathbf{w}(n-1)\hat{\mathbf{w}}^*(n-1)\mathbf{x}(n-1)\mathbf{x}^*(n-1)\boldsymbol{\alpha}(n-1)\right] \\ &= E\left[\mathbf{w}(n+1)\hat{\mathbf{w}}^*(n-1)\right].\left[\mathbf{I} - \mathbf{R}(n-1)\boldsymbol{\alpha}(n-1)\right] \\ &\quad + \mathbf{R}_{\mathbf{w}}(2)\mathbf{R}(n-1)\boldsymbol{\alpha}(n-1).\end{aligned} \tag{A.19}$$

Iterating (A.19) (n-1) times, we obtain

$$\begin{aligned}E\left[\mathbf{w}(n+1)\hat{\mathbf{w}}^*(n)\right] &= \mathbf{R}_{\mathbf{w}}(2)\mathbf{R}(n-1)\boldsymbol{\alpha}(n-1) \\ &\quad + \sum_{k=1}^{n-1}\mathbf{R}_{\mathbf{w}}(k+2)\mathbf{R}(n-k-1)\boldsymbol{\alpha}(n-k-1) \\ &\quad .\prod_{j=k}^{1}\left[\mathbf{I} - \mathbf{R}(n-j)\boldsymbol{\alpha}(n-j)\right].\end{aligned} \tag{A.20}$$

Similarly,

$$\begin{aligned}E\left[\mathbf{w}(n)\hat{\mathbf{w}}^*(n)\right] &= \mathbf{R}_{\mathbf{w}}(1)\mathbf{R}(n-1)\boldsymbol{\alpha}(n-1) \\ &\quad + \sum_{k=1}^{n-1}\mathbf{R}_{\mathbf{w}}(k+1)\mathbf{R}(n-k-1)\boldsymbol{\alpha}(n-k-1) \\ &\quad .\prod_{j=k}^{1}\left[\mathbf{I} - \mathbf{R}(n-j)\boldsymbol{\alpha}(n-j)\right]\end{aligned} \tag{A.21}$$

On substituting (A.20) and (A.21) in (A.18), we obtain

$$\begin{aligned}\mathbf{\Gamma} &= E\left[\left(\mathbf{w}(n+1) - \mathbf{w}(n)\right)\mathbf{v}^*(n)\right] \\ &= \left[\mathbf{R}_w(1) - \mathbf{R}_w(0)\right] - \mathbf{R}_w(2)\mathbf{R}(n-1)\boldsymbol{\alpha}(n-1) \\ &\quad - \sum_{k=1}^{n-1}\mathbf{R}_{\mathbf{w}}(k+2)\mathbf{R}(n-k-1)\boldsymbol{\alpha}(n-k-1)\prod_{j=k}^{1}\left[\mathbf{I} - \mathbf{R}(n-j)\boldsymbol{\alpha}(n-j)\right] \\ &\quad + \mathbf{R}_w(1)\mathbf{R}(n-1)\boldsymbol{\alpha}(n-1) \\ &\quad + \sum_{k=1}^{n-1}\mathbf{R}_w(k+1)\mathbf{R}(n-k-1)\boldsymbol{\alpha}(n-k-1)\prod_{j=k}^{1}\left[\mathbf{I} - \mathbf{R}(n-j)\boldsymbol{\alpha}(n-j)\right]\end{aligned}$$

$$\begin{aligned}\mathbf{\Gamma} &= \left[\mathbf{R}_w(1) - \mathbf{R}_w(0)\right] + \left[\mathbf{R}_w(1) - \mathbf{R}_w(2)\right]\mathbf{R}(n-1)\boldsymbol{\alpha}(n-1) \\ &\quad + \sum_{k=1}^{n-1}\left[\mathbf{R}_{\mathbf{w}}(k+1) - \mathbf{R}_{\mathbf{w}}(k+2)\right]\mathbf{R}(n-k-1)\boldsymbol{\alpha}(n-k-1) \\ &\quad .\prod_{j=k}^{1}\left[\mathbf{I} - \mathbf{R}(n-j)\boldsymbol{\alpha}(n-j)\right].\end{aligned} \tag{A.22}$$

Therefore,

$$\begin{aligned}\mathrm{Tr}\left[\mathbf{\Gamma}\right] &= \mathrm{Tr}\left[\mathbf{R}_{\mathbf{w}}(1) - \mathbf{R}_{\mathbf{w}}(0)\right] + \gamma \mathrm{Tr}\left[\mathbf{R}_{\mathbf{w}}(1) - \mathbf{R}_{\mathbf{w}}(2)\right] \\ &\quad + \sum_{k=1}^{n-1}\gamma(1-\gamma)^k \mathrm{Tr}\left[\mathbf{R}_{\mathbf{w}}(k+1) - \mathbf{R}_{\mathbf{w}}(k+2)\right].\end{aligned} \tag{A.23}$$

On substituting (A.23) in (A.17) and taking trace on both the sides, we obtain

$$\begin{aligned}\mathrm{Tr}\left[\mathbf{K}_p(n)\right] &= 2\mathrm{Tr}\left[\mathbf{R}_{\mathbf{w}}(0) - \mathbf{R}_{\mathbf{w}}(1)\right] + D(n) + 2\mathrm{Tr}\left[\mathbf{\Gamma}\right] \\ &= D(n) + 2\gamma \mathrm{Tr}\left[\mathbf{R}_{\mathbf{w}}(1) - \mathbf{R}_{\mathbf{w}}(2)\right] \\ &\quad + \sum_{k=1}^{n-1}\gamma(1-\gamma)^k \mathrm{Tr}\left[\mathbf{R}_{\mathbf{w}}(k+1) - \mathbf{R}_{\mathbf{w}}(k+2)\right].\end{aligned} \tag{A.24}$$

Likewise, computing for $\tilde{\mathbf{K}}_p(n)$,

$$\tilde{\mathbf{K}}_p(n) = E\left[\left(\mathbf{w}(n+1) - \mathbf{w}(n) + \mathbf{v}(n)\right)\mathbf{v}^*(n)\right] = \mathbf{\Gamma} + \mathbf{K}(n) \tag{A.25}$$

Taking the trace of (A.25), we obtain

$$\begin{aligned}&\mathrm{Tr}\left[\tilde{\mathbf{K}}_{\mathrm{p}}(n)\right]=D(n)+\mathrm{Tr}[\boldsymbol{\Gamma}]\\&=D(n)+\mathrm{Tr}\left[\mathbf{R}_{\mathrm{w}}(1)-\mathbf{R}_{\mathrm{w}}(0)\right]+\gamma\mathrm{Tr}\left[\mathbf{R}_{\mathrm{w}}(1)-\mathbf{R}_{\mathrm{w}}(2)\right]\\&\quad+\sum_{k=1}^{n-1}\gamma(1-\gamma)^{k}\,\mathrm{Tr}\left[\mathbf{R}_{\mathbf{w}}(k+1)-\mathbf{R}_{\mathbf{w}}(k+2)\right]. \qquad (A.26)\end{aligned}$$

On substituting (A.24) and (A.26) in (A.16), we get

$$\begin{aligned}\left(1-\gamma^{2}\right)D(n)&=\gamma\left\{J_{\mathrm{ex}}(n)+\sigma_{c}^{2}\right\}\mathrm{Tr}\left[\boldsymbol{\Lambda}_{\boldsymbol{\alpha}}(n)\right]\\&\quad+D(n)+2\gamma\mathrm{Tr}\left[\mathbf{R}_{\mathbf{w}}(1)-\mathbf{R}_{\mathbf{w}}(2)\right]\\&\quad+\sum_{k=1}^{n-1}\gamma(1-\gamma)^{k}\,\mathrm{Tr}\left[\mathbf{R}_{\mathbf{w}}(k+1)-\mathbf{R}_{\mathbf{w}}(k+2)\right]\\&\quad-2\gamma D(n)-2\gamma\mathrm{Tr}\left[\mathbf{R}_{\mathbf{w}}(1)-\mathbf{R}_{\mathbf{w}}(0)\right]\\&\quad-2\gamma^{2}\mathrm{Tr}\left[\mathbf{R}_{\mathbf{w}}(1)-\mathbf{R}_{\mathbf{w}}(2)\right]\\&-2\sum_{k=1}^{n-1}\gamma^{2}(1-\gamma)^{k}\,\mathrm{Tr}\left[\mathbf{R}_{\mathbf{w}}(k+1)-\mathbf{R}_{\mathbf{w}}(k+2)\right].\end{aligned}$$

(A.27)

On simplifying (A.27), we obtain

$$\begin{aligned}D(n)&=\frac{1}{2(1-\gamma)}\left\{J_{\mathrm{ex}}(n)+\sigma_{c}^{2}\right\}\mathrm{Tr}\left[\boldsymbol{\Lambda}_{\boldsymbol{\alpha}}(n)\right]\\&+\sum_{k=0}^{n-1}(1-\gamma)^{k}\,\mathrm{Tr}\left[\mathbf{R}_{\mathbf{w}}(k+1)-\mathbf{R}_{\mathbf{w}}(k+2)\right]\\&\qquad+\frac{1}{(1-\gamma)}\mathrm{Tr}\left[\mathbf{R}_{\mathbf{w}}(0)-\mathbf{R}_{\mathbf{w}}(1)\right]. \qquad (A.28)\end{aligned}$$

References:

[1] Bernard Sklar, "Rayleigh fading channels in mobile digital communication systems Part-I: Characterization," *IEEE Communications Magazine*, pp. 90-100, July 1997.

[2] D. Tse and P. Viswanath, Fundamentals of Wireless Communication, Cambridge University Press, 2005.

[3] J. F. Galdino, and E. L. Pinto, "A simulation study of adaptive filtering applied to MLSE-PSP receivers," in *Proceedings of IEEE Military Communications Conference*, MILCOM 1998, pp. 338-342 vol.1.

[4] J. F. Galdino, E. L. Pinto, and M. S. de Alencar, "Analytical performance of the LMS algorithm on the estimation of wide sense stationary channels," *IEEE Transactions on Communications*, vol. 52, no. 6, pp. 982-991, 2004.

[5] L. Lindbom, A. Ahlén, M. Sternad, and M. Falkenstrom, "Tracking of time-varying mobile radio channels—Part II:Acase study," *IEEE Trans. Commun.*, vol. 50, pp. 156-167, Jan. 2002.

[6] L. Lindbom, M. Sternad, and A. Ahlén, "Tracking of time-varying mobile radio channels—Part I: The Wiener LMS algorithm," *IEEE Trans. Commun.*, vol. 49, pp. 2207-2217, Dec. 2001.

[7] C. Cao, L. Xie, H. Zhang, S. Xie, "A robust channel estimator for DS-CDMA systems under multipath fading channels," *IEEE Transactions on Signal Processing*, vol.54, no.1, pp. 13- 22, Jan. 2006.

[8] Q. Nasir, "Wireless Channel Tracking Based on Optimum Predictive LMS," *Wireless Personal Communications*, vol. 48, no. 4, pp. 511-519, 2009.

[9] A. Jamoos, W. Bobillet, E. Grivel, H.A. Nour, and M. Najim, "Identification of Time-Varying Frequency-Flat Rayleigh Fading Channels Based on Errors-In-Variables Approach," *IEEE 7th Workshop on Signal Processing Advances in Wireless Communications, 2006. SPAWC '06*, vol., no., pp.1-5, 2-5 July 2006.

[10] B. Chen, Y. Chung, and D. Huang, "A Wavelet Time-Scale Deconvolution Filter Design for Nonstationary Signal Transmission Systems through a Multipath Fading Channel", *IEEE Transactions on Signal Processing*, vol. 47, no. 5, pp. 1441-1446, 1999.

[11] B. S. Chen, and C. W. Lin, "Multiscale Wiener filter for the restoration of the fractal signal: Wavelet filter bank approach," *IEEE Trans. Signal Processing*, vol. 42, pp. 2972–2982, 1994.

[12] G. W. Wornell, "A Karhunen–Lo`eve expansion for 1=f processes via wavelets," *IEEE Trans. Inform. Theory*, vol. 36, pp. 859–861, 1990.

[13] G. S. Wornell and A. V. Oppenheim, "Estimation of fractal signals from noisy measurements using wavelets," *IEEE Trans. Signal Processing*, vol. 40, pp. 611–623, 1992.

[14] E. Masery, "The wavelet transform of stochastic processes with stationary increments and its application to fractional Brownian motion," *IEEE Trans. Inform. Theory*, vol. 39, pp. 260–264, 1993.

[15] A. Gupta, and S. Joshi, "Variable Step-Size LMS Algorithm for Fractal Signals," *IEEE Transactions on Signal Processing*, vol. 56, no. 4, pp. 1411-1420, 2008.

[16] E. Perrin, R. Harba, C. B. Joseph *et al.*, "nth-order Fractional Brownian Motion and Fractional Gaussian Noises," *IEEE Transactions on Signal Processing*, vol. 49, no. 5, pp. 1049-1059, May 2001.

[17] B. Widrow, J. M. McCool, M. G. Larimore *et al.*, "Stationary and Non-stationary Learning characteristics of the LMS Adaptive Filter," *Proceedings of IEEE*, vol. 64, pp. 1151-1162, Aug. 1976.

[18] A. Gupta, and S. Joshi, "Some Studies on the Structure of Covariance Matrix of Discrete-Time fBm," *IEEE Transactions on Signal Processing*, vol. 56, no. 10, pp. 4635-4650, 2008.

[19] P. A. Bello, "Characterization of randomly time-variant linear channels," IEEE Trans. Comm. Syst., vol. 11, pp. 360–393, 1963.

[20] P. Höher, "A statistical discrete-time model for the WSSUS multipath channel," *IEEE Trans. Veh. Technol.*, vol. 41, no. 4, pp. 461–468, Jul. 1992.

[21] S. Haykins and T. Kailath, Adaptive Filter Theory, Pearson Education, Inc., 2002.

[22] J. D. Parsons, *The Mobile Radio Propagation Channel*. New York: Wiley, 1992.

[23] W. C. Jakes, *Microwave Mobile Communications*. Wiley, 1974, re-issued by IEEE Press, 1994.

[24] A. Gupta and S.D. Joshi, "Estimation of an Asymptotically Stationary AR Channel Using fBm Based LMS Algorithm," *IEEE International Conference on Signal Processing & Communications*, SPCOM-2012, 22-25 July, 2012, IISc Bangalore, India.

[25] K. Baddour and N. Beaulieu, "Autoregressive modeling for fading channel simulation," *Wireless Communications, IEEE Transactions on*, vol. 4, no. 4, pp. 1650–1662, Jul 2005.